

Recoverable Compliance Behavior of High-Density Polyethylenes

DONALD J. PLAZEK and N. RAGHUPATHI, *Department of Metallurgical and Materials Engineering, University of Pittsburgh, Pittsburgh, Pennsylvania 15261*, and ROBERT F. KRATZ and WILLIAM R. MILLER, JR., *Arco/Polymers, Monaca, Pennsylvania 15061*

Synopsis

Eight samples of high-density polyethylene with weight-average molecular weights ranging from 5.5×10^4 to 17.3×10^4 have been studied. In addition to GPC molecular weight characterization, the recoverable compliance, the shear viscosity, and the extrudate swell were determined at temperatures between 138 and 200°C. The range of the maximum creep stresses ranged from 60 to 1840 dynes/cm². The creep recovery response was in the linear or near-linear range. The results are interpreted in the light of the anomalous results of Mendelson and Finger.

INTRODUCTION

The Newtonian fluid and the perfectly elastic solid are limiting idealized models of material behavior. The Newtonian fluid model closely represents the response of low-viscosity liquids to shearing stresses over wide ranges of shear rate and frequency, and the perfectly elastic solid approximates the linear stress-strain response of spring metals like phosphor-bronze and beryllium-copper alloys and tempered steel. There are of course limits to the adherence to these models. Relaxation phenomena can be observed in many liquids at high frequencies of excitation and anelastic effects, commonly called internal friction, are easily noted in the damped vibrations of metals. These phenomena reflect a time or frequency dependence in the response of the materials which can be described at low rates of shear and small strains by the well-developed linear theory of viscoelasticity that is based on Boltzmann's linear superposition principle.^{1,2}

Viscoelastic response is often most dramatically displayed by high polymers where an extreme time dependence of response is unavoidable. The linear time-dependent response is a more general behavior encompassing the Newtonian liquid model and perfectly elastic solid model as limiting forms at long times and short times, respectively. However, it does not appear profitable to consider a viscoelastic response as partly a liquid-like response and partly a solid-like response. In fact, confusion can arise from such a viewpoint. The more general viscoelastic model handles all these forms of response with a completely internal consistency just so long as the material of interest has been shown to obey Boltzmann superposition. In this sense the structure of linear viscoelasticity is as sound and complete a "cathedral" as that of equilibrium thermodynamics.³

The viscoelastic functions, the complex dynamic shear compliance J^* and the shear creep compliance $J(t)$, each readily indicate how much of a deformation

is permanent by virtue of a viscous flow contribution and how much is recoverable as a function of time. It is therefore not necessary and indeed not advisable to refer to liquid, rubbery, or glassy states of a polymer when referring to a viscoelastic response curve. The material giving rise to the response at a given temperature is either a viscoelastic liquid or solid (depending on whether it flows or not) and is at all times in one state, if it is completely amorphous. It appears to be glassy, rubbery, or liquid depending on how fast or slowly you look at it.

Beyond the domain of linear viscoelasticity lies a family of nonlinear effects (non-Newtonian flow, normal stresses, strain-dependent memory functions, and stress-dependent plastic deformation) which calls for a more intricate and complicated structure than linear viscoelasticity. These effects and models, of course, are being continually investigated.

The above points have been made to discourage the use of the ill-defined concept of "melt elasticity" when linear viscoelastic functions or nonlinear counterparts are needed. It seems that the intervention of complicating geometric effects such as are encountered in extrusion processes lure or seduce investigators away from well-established forms of the mechanical characterization of polymers.

One can operate from the point of view that ultimately the theory or theories of nonlinear viscoelasticity will be able to completely explain the phenomena of extrudate swell, "melt fracture," and the presence and nature of normal stresses.

The recoverable compliance $J_r(t)$, which can be measured directly from the recoverable deformation following steady-state creep, is

$$J_r(t) = J(t) - t/\eta = J_g + J_d \psi(t) \quad (1)$$

where t is the time (sec), J_g is the glassy compliance, J_d is the delayed recoverable shear compliance, and $\psi(t)$ is the normalized retardation function; $\psi(0) = 0$ and $\psi(\infty) = 1$; $J_g + J_d = J_e$, the steady-state recoverable compliance. It has been well established that J_r at relative long times approaching steady-state behavior increases with molecular weight and molecular weight distribution,^{4,5} except for narrow-distribution polymers with molecular weights greater than ca. 10^5 , where J_e is sensibly constant.⁶⁻⁹ The molecular origin for the recoverable deformation observed in creep is the orientation of the polymer molecules. Thermal energy in the form of Brownian motion drives the molecular conformations back toward their most random state, with rates being controlled by the density of the polymer. This molecular orientation similarly is responsible for extrudate swell and the normal forces generated in the nonlinear regime of response. In fact, the relation between J_e and the first normal stress difference is known for a second-order fluid¹⁰:

$$\eta_0^2 J_e = (p_{11} - p_{22})/2\dot{\gamma}^2 \quad (2)$$

where η_0 is the limiting low rate-of-shear viscosity, $p_{11} - p_{22}$ is the steady-state first normal stress difference, and $\dot{\gamma}$ is the shear rate. At higher strain rates beyond the second-order fluid behavior, this simple relationship fails.¹¹ Extrudate swell is a complicated form of unconstrained* recovery which one would expect to be related to J_e if the extrudate were in viscoelastic steady-state shear as it emerged from the capillary die, i.e., $\psi(t) = 1$.

* In the usual recovery experiment the sample is constrained between instrumental surfaces, e.g., parallel plates, a cone and a plate, or cylindrical surfaces.

EXPERIMENTAL

The eight materials employed in this study were commercial high-density polyethylenes from three sources: from Dow Chemicals, Dow 18060; from Allied Chemicals, Allied 55-100; and from ARCO/Polymers, six Super Dylan (SD) polyethylenes types 605, 6550, 6560, 7007, 7006, and 7002.

The principal characterization was gel permeation chromatography (GPC).¹³ Short-chain branching was obtained by infrared analysis. These data are given in Table I.

Instron capillary rheometry was performed at 190°C and at cross-head speeds between 0.01 and 20.0 in./min. Since the tungsten carbide capillary was 2.005 in. long and 0.0502 in. in diameter and the plunger was 0.3746 in. in diameter, the above cross-head speeds correspond to a range of apparent shear rate of 1.48 and to 2960 sec⁻¹. However, in fitting the Sabia equation¹⁴ to the data, only points between 0.05 and 5.0 in./min cross-head speeds were employed. For polyethylenes, the Sabia equation is

$$\log \frac{\eta}{\eta_0} = \left(\frac{\eta}{\eta_0} - 2 \right) \log \left[1 + \left(\frac{\dot{\gamma}}{\dot{\gamma}_0} \right)^{1/3} \right] \quad (3)$$

where η is the viscosity, $\dot{\gamma}$ is the shear rate, η_0 is the zero shear viscosity, and $\dot{\gamma}_0$ is the characteristic shear rate. These data are also shown in Table I.

Some of our most extended measurements required that the polyethylene samples be kept above their melting temperature for as long as a week. To obtain the necessary stability under rough vacuum conditions (ca. 10⁻² torr), it was necessary to add 0.1% Santonox antioxidant, 4,4'-thiobis(6-*t*-butyl-*m*-cresol). The Santonox was graciously provided by R. A. Mendelson. Its uniform distribution was accomplished in xylene solution followed by reduced pressure distillation in a rotovaporator.

Mendelson and Finger¹² have reported that the *compliance* of molten high-density polyethylene (HDPE) *decreases* with *increasing molecular weight and increasing breadth of the molecular weight distribution*. The compliances reported were calculated from extrudate swell data obtained on an extensive and varied series of HDPE samples. A relatively long capillary (length/diameter = 40) was used in the extrusion measurements, so entrance end effects were assumed to be negligible. Apparently, viscoelastic steady-state conditions were also assumed, otherwise a unique compliance could not be reported. The recoverable shear compliance of a viscoelastic liquid such as molten polyethylene is a function of the time of shearing which ultimately reaches a long-time limiting characterizing value, see Figure 1.

Since this and other assumptions were necessary to obtain the shear compliances from extrudate swell values, it seemed desirable to check the startling conclusions with direct measurements of the linear and nonlinear viscoelastic response. The shear creep and creep recovery results we have obtained so far and are reporting here are in the linear and near-linear range of response of a series of eight HDPE samples. Mendelson and Finger's samples ranged in weight-average molecular weight M_w from 8.3×10^4 to 4.1×10^5 . Heterogeneity ratios M_w/M_n extended from 4.7 to 28, and M_z/M_w ratios, from 5.0 to 14. The M_w values of our samples range from 5.5×10^4 to 1.7×10^5 ; M_w/M_n ratios extend from 3.4 to 12; and M_z/M_w ratios, from 2.4 to 9.7. While our sample range tends to extend to lower molecular weights and Mendelson and Finger's extend to

TABLE I
High-Density Polyethylenes

Material	Molecular weights by GPC				Short-chain branching by IR, branches per 10 ³ C atoms	Sabia parameters for 190°C	
	$M_n \times 10^{-3}$	$M_w \times 10^{-3}$	$M_z \times 10^{-3}$	M_w/M_n		M_z/M_w	η_0 , kP
Dow 18060	6.9	55	209	8.0	3.8	7.7	240
Allied 55-100	13	65	257	5.0	4.0	9.7	280
SD 605	8.7	73	704	10.4	10.8	26	18
SD 6550	22	74	178	3.4	2.4	24	220
SD 6560	13	94	646	7.2	6.9	18	96
SD 7007	11	125	884	11.4	7.1	180	3.0
SD 7006	13	155	1318	11.9	8.5	190	2.4
SD 7002	15	173	1200	11.5	6.9	570	0.88

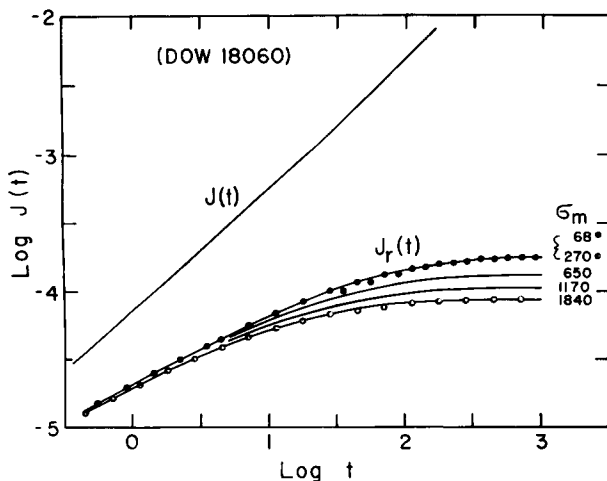


Fig. 1. Logarithmic creep $J(t)$ and creep recovery $J_r(t)$ curves of a high-density polyethylene, Dow 18060 ($M_w = 55,000$) presented as a function of the logarithmic time. Results for a range of maximum stress levels σ_m extending from 68 to 1840 dynes/cm² are shown. Temperature of measurements was 138°C.

slightly higher values, there is considerable overlap. In addition, the trends reported here would only be exaggerated at higher molecular weights.

RESULTS

During the first phase of our investigations into the linear and nonlinear viscoelastic response of commercial high-density polyethylene (HDPE) samples it was desired to limit measurements of shear creep and creep recovery to the linear range of response. This was not possible since the linear range of response of the higher molecular weight samples was not within our experimental range in spite of the fact that our lowest stress levels were about 60 dynes/cm². A torsional creep instrument¹⁵ was used in carrying out the creep and recovery measurements at temperatures between 136° and 187°C. Samples of circular cross section were twisted between flat platens. Most of the coin-shaped samples were 6 mm in diameter, with heights between 1.5 and 2.0 mm. Values of the stress reported here are maximum values found at the outer radius of the sample.

Shear rates were sufficiently low so that decreases in the measured viscosity from η_0 with increasing rate of shear were less than 10%, in most cases less than 2%, where η_0 is the limiting low rate of shear value of the shear viscosity. Creep $J(t)$ and recoverable compliance $J_r(t)$ values have been calculated as if the response were completely linear. Virtually no error was incurred in representing viscous contributions to the deformation. At short times, the recoverable compliance is uniquely represented because the response is indeed linear, and therefore no error resulting from variation of the stress in the sample is present. In the terminal region of response the apparent recoverable compliance decreases with increasing stress level and increasing strain rate. This kind of behavior has been seen before^{7,11,16-19} and is illustrated by the response at 138°C of a Dow HDPE material designated 18060 shown in Figure 1. The maximum shearing

stress in the sample during creep was $\sigma_m = 2M/\pi R^3$, where M is the torque (dynes-cm) and R (cm) is the radius of the right circular cylinder. The behavior observed must be noted to be somewhat unusual since the response is sensibly linear during creep and appreciably nonlinear during recovery. The linearity during creep results from the fact that at short times and small strains the recoverable component of the deformation is linear; and at long times where the recoverable component is not linear, the viscous contribution to the deformation, t/η , dominates, and $\eta \cong \eta_0$. Assuming that the stress at all points within the cylindrical sample is constant in time (not radius) when the applied torque is held constant, the following expression can be derived²⁰ to yield nonlinear creep compliance $J(\sigma, t)$. The derivation is analogous to that of Weissenberg for nonlinear laminar flow in a tube.¹⁰ At a given time t of creep,

$$J(\sigma, t) = 2\pi R^4 \theta(t)/ML \left[\left(\frac{\partial \log \sigma_m}{\partial \log \gamma_m(t)} \right)_t + 3 \right] \quad (4)$$

where R is the radius and L is the length of the right circular cylinder, $\theta(t)$ is the time-dependent angle of twist, M is the applied torque, σ_m is the stress at the outer surface, and γ_m is the corresponding strain. The above derivative has a value of 1 in the linear range of response and decreases for the usual kind of nonlinearity in creep, i.e., $J(\sigma, t)$ increases with increasing strain rate because of the diminishing viscosity. However, we would expect the correction term for the *nonlinear recoverable compliance*, $J_r(\sigma, t)$, to increase from a value of 4 instead of dropping from 4 toward 3. The opposing corrections are the result of the fact that while the viscosity decreases with increasing shear rate, yielding larger contributions to the creep deformation, the recoverable deformation is diminished in the terminal regions of response. The derivative of the creep stress relative to the recoverable strain should therefore be used. A plot of the maximum creep stress (i.e., the value at the cylindrical surface of the sample) σ_m versus the maximum recoverable strain $\gamma_{r,m}(t)$ for the Dow 18060 PE is shown in Figure 2, where the slope rises from a value of 1 to 2. Steady-state creep preceded each pertinent recovery experiment, and the time chosen for this plot was effectively infinite (see Fig. 1; $\log t = 3$), i.e., after complete recovery.

It is important to note again explicitly that not only does the nonlinearity of the recovery become apparent at lower stress levels and strain rates than non-Newtonian flow, but that the two deviations from linear behavior are opposed in contributing to creep deformation. The recoverable deformation, obtained in recovery experiments which follow nonsteady-state creep, $\theta < \infty$, can in general be larger than that following steady-state creep at the same stress levels.²¹ Such behavior is expected from materials that show the stress overshoot effect.¹¹ It should also be noted that because of various *changes in material response with the time of creep*, including the viscosity decrease, the stress distribution in a *right circular cylinder* with an applied constant torque changes with time. It is therefore conceptually impossible to carry out a rigorous creep experiment on such a polymer specimen responding in a nonlinear manner, i.e., the stress cannot be kept constant.* For example, considering only a viscous response, the viscosity has its limiting low rate-of-shear value immediately after a shearing

* Of course, such nonlinear creep and recovery measurements can be carried out using geometrical arrangements where the rate of shear is approximately constant throughout the sample (e.g., cone and plate or small gap Couette geometries).

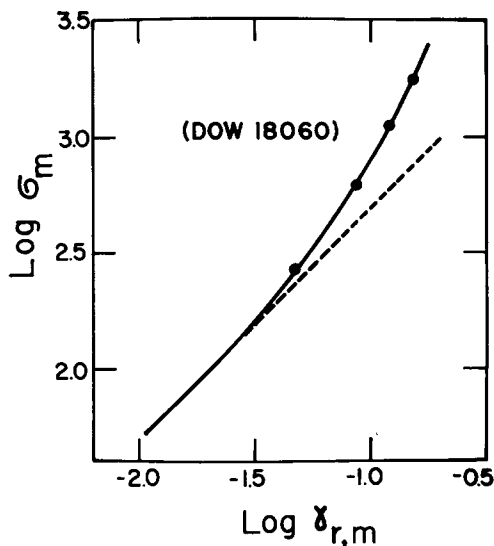


Fig. 2. Logarithmic plot of the maximum sample creep stress σ_m vs. total recoverable strain found at the cylindrical surface of the sample, $\gamma_{r,m}$. Values corresponding to the steady-state limits seen in Figure 1. This is the long-time limiting stress-strain curve for the recoverable deformation of the Dow 18060 high-density polyethylene. Temperature of measurement was 138°C.

traction is applied even if the ensuing rates of shear are mostly in the non-Newtonian range for the material under investigation. At such a moment the response is linear, and the shearing stress at any point within the right circular cylinder is $\sigma(r) = 2Mr/\pi R^4$, where r is the radius of the point. At a later time the viscosity of the material near the maximum radius experiences the greatest decrease as a result of a decrease in entanglement concentration because the rate of shear is the largest at the outer edge. Hence, under conditions of constant torque the load borne by the outermost material is reduced as its viscosity falls. The stress distribution is not the same when part of the material being sheared torsionally between two circular platens is not responding linearly. Our recoverable compliance curves are therefore to be considered approximate in the nonlinear region of response. Under the most extreme conditions we estimate that the recoverable compliance values are not more than 25% too high. In Figure 1 the points at the longest times following creep at the highest stress level probably should be depressed by an additional 0.1 logarithmic unit. Therefore, any nonlinear effects we have observed may be underestimated.

With the help of Figure 1 and the fact that creep times preceding the indicated recovery measurements on the Dow 18060 HDPE were 1000 sec or greater, one can conclude that linear behavior in recovery was approached at the lowest creep stress levels and that the preceding creep deformations achieved steady state. The longest time indicated to achieve full recovery is about 1000 sec. When steady state is not achieved in a creep measurement, the subsequent time for complete recovery will always be greater than the time of creep.

The nonlinear steady-state recoverable compliance levels $J_e(\sigma)$ for three of the lowest molecular weight samples, including the Dow 18060, are shown in Figure 3. The extrapolations to linear behavior were aided by a reduction procedure which will be reported in the future. The responses of the higher molecular weight samples were further removed from linearity.

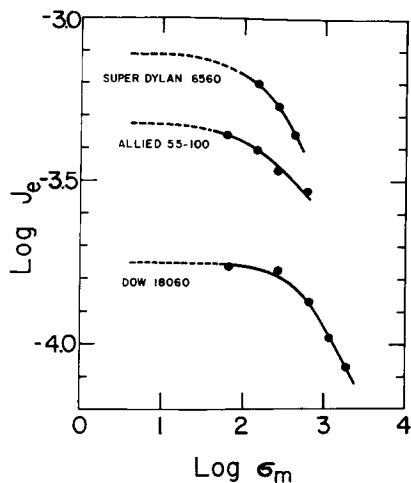


Fig. 3. Logarithmic plots of the steady-state recoverable compliance J_r for three of the high-density polyethylenes studied as a function of the maximum creep stress of the samples. Estimated extrapolations to the linear range of response are shown. Temperature of measurement was 138°C.

One of the most significant features of the nonlinear rheological response of polymers is the elimination of viscoelastic mechanisms with the longest relaxation or retardation times.²²⁻²⁴ Steady-state viscoelastic response is therefore reached at shorter times. In terms of the retardation spectrum, the long-time tail is truncated. To indicate the extent of the curtailment of the long-time response, the time t_c at which the slope $d \log [J_r(t)]/d [\log t]$ has decreased to 0.10 is plotted logarithmically in Figure 4 as a function of σ_m . A relationship close to inverse proportionality is indicated at the highest stress levels. In the linear region of response, of course, the slopes of the recoverable compliance curves are independent of the stress level.

Since the kind of nonlinearity reported here is widely observed, we wished to see how and to what extent the other viscoelastic functions are affected. Strictly

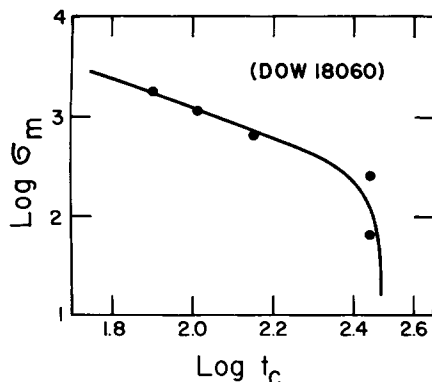


Fig. 4. Time of recovery t_c where the slope of the logarithmic recovery curve reaches a value of 0.1 (from Fig. 1) plotted logarithmically versus maximum creep stress in the sample. A decrease in t_c reflects a curtailment of the terminal viscoelastic response of the material. Temperature of measurement was 138°C.

speaking, the transformation of the nonlinear response curves cannot be made in general with any of the relations from linear viscoelasticity. However, we believe that the nonlinear recovery that we have observed following steady-state creep approximates closely the linear response that would be observed if small stresses or deformations were superimposed on an independent steady shearing. The measurements of Simmons and Tanner^{22,23} provide an example of such measurements, and the analysis of Markovitz provides the rationale for the applicability of the relations of linear viscoelasticity.²⁵ From a molecular point of view, we believe that a steady shearing field applied to a high polymer or its solutions at sufficiently high rates of shear alters both the number and the *distribution* of the molecular entanglements. Thus, the sheared polymeric sample can be considered a different material which can respond linearly to small applied tractions or deformations. This response characterizes its altered state. Our recovery measurements follow such steady-state shearing and should in large measure characterize the altered state of the material. Since the recoverable deformation reflects the degree of orientation existing before the start of the recovery, it is not likely that the additional entanglements, formed in reestablishing the "at rest" level concentration of entanglements, should affect the measured recovery. Perhaps the rate of recovery in the far terminal region might show a secondary effect. This proposition relating nonlinear recovery to superimposed deformations is subject to future experimental verification.

Assuming the hypothesis is correct, we have applied the following approximate relations²⁶ to calculate the real and imaginary components J' and J'' of the complex dynamic compliance J^* (cm²/dyne) from the recoverable compliance and the viscosity:

$$J'(\omega) \cong [1 - m(2t)]^{0.8} J_r(t) \quad (5)$$

$$J''(\omega) - 1/\omega\eta \cong [m(2t/3)]^{0.8} J_r(t) \quad (6)$$

where the time t (sec) is equal to the reciprocal of the angular frequency $1/\omega$ (sec/rad) and m is $d[\log J_r(t)]/d[\log t]$. In Figure 5 the results of the calculations are shown for the linear results and those on the recovery results following creep with $\sigma_m = 1840$ dynes/cm². For the same reasons that there is effectively only one creep compliance curve, there is only one J'' curve. However, the imaginary component sans contribution from viscous deformation $J''(\omega) - (1/\omega\eta)$ shows a much greater reflection of the nonlinearity than does $J'(\omega)$.

The compliances were transformed into components of the complex dynamic rigidity $G^* = G' + iG''$ by means of their algebraic relations

$$G'(\omega) = J'(\omega)/[J'(\omega)^2 + J''(\omega)^2] \quad (7)$$

$$G''(\omega) = J''(\omega)/[J'(\omega)^2 + J''(\omega)^2] \quad (8)$$

The effect on the corresponding stress relaxation modulus, $G(t)$, was estimated using the expression of Ninomiya and Ferry²⁷

$$G(t) = G'(\omega) - 0.40G''(0.40\omega) + 0.014G''(10\omega)|_{\omega=t^{-1}}$$

The results are all shown in Figure 6, where the apparently paradoxical effect of the nonlinearity results in a diminution of the values of the real component of the complex dynamic modulus $G'(\omega)$, in addition to a similar decrease in $J'(\omega)$ seen in Figure 5. We have an instance here where discussion in terms of ap-

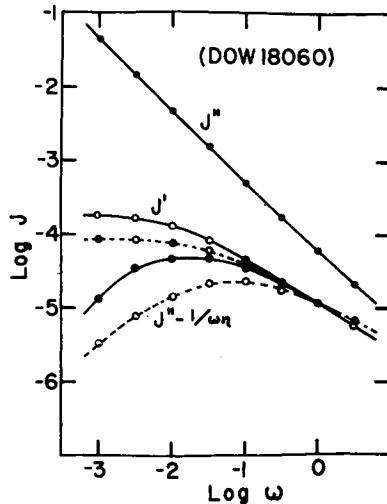


Fig. 5. Components of the dynamic shear compliance, $J'(\omega)$ and $J''(\omega)$, shown plotted logarithmically vs. the logarithmic angular frequency ω . The imaginary component without viscous deformation contributions, $J'' - 1/\omega\eta$, is also shown. Solid lines represent the linear response, dashed lines represent the nonlinear response when $\sigma_m = 1840$ dynes/cm². See text for details. Temperature of measurement was 138°C.

proximate layman's language is not possible, i.e., the material becomes softer and harder at the same time. Mathematically, this result becomes obvious when one notes that in the far terminal region $J'' \gg J'$ and $J'' \cong 1/\omega\eta$ eqs. (7) and (8) become

$$G' = J'\omega^2\eta^2 \quad (9)$$

$$G'' = \omega\eta \quad (10)$$

Therefore, with fixed η , as is our case here, a decrease in J' demands a decrease in G' at a given ω . We believe that we have in this instance an argument for looking to compliance functions when attempting molecular interpretations. There is no doubt that a decrease in $J_r(t)$ or $J'(\omega)$ reflects a decrease in the amount of orientation per unit stress; but since G' is very sensitive to η , no conclusions are immediately obvious. It has been noted that a plateau can be seen in $J(t)$ when it is clear there is no rubbery plateau indicated by $J_r(t)$ or the retardation spectrum.²⁸ Unpublished calculations on the data reported in reference 29 also show that such misleading plateaus are more pronounced in the modulus curves.

It is obvious from eq. (9) that the decrease in the values of G' with increasing shear stress are proportional to that of the J' values, but they appear to be smaller because of the higher absolute slopes of the log G' curve. The stress relaxation modulus $G(t)$ apparently is the most severely diminished viscoelastic function by the onset of the observed nonlinearity.

In contrast to the behavior of the lowest molecular weight HDPE material being reported here, Figure 7 displays the fact that steady-state behavior of one of the higher molecular weight samples, SD 7006, was not attainable at a creep stress of $\sigma_m = 150$ dynes/cm²; $T = 138^\circ\text{C}$. The preceding creep time θ was 112 hr ($\log \theta = 5.60$). It can be seen that a higher temperature of 180°C is of little help in achieving steady state. The somewhat lower terminal slope at 180°C

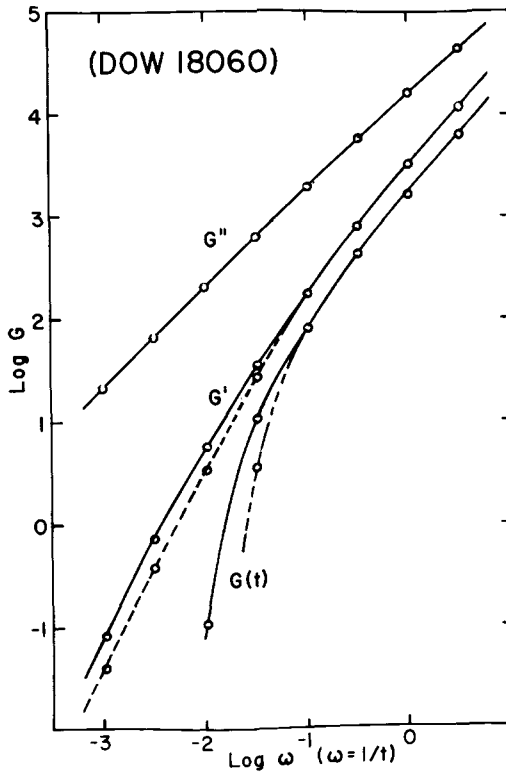


Fig. 6. Components of the dynamic shear modulus, $G'(\omega)$ and $G''(\omega)$ shown plotted logarithmically vs. the logarithm of the angular frequency ω . Stress relaxation modulus is also shown plotted against $-\log t$. Solid lines represent the linear response of the Dow 18060 polyethylene, and the dashed lines, the nonlinear response where $\sigma_m = 1840$ dynes/cm². See text for calculation details. Temperature of measurement was 138°C.

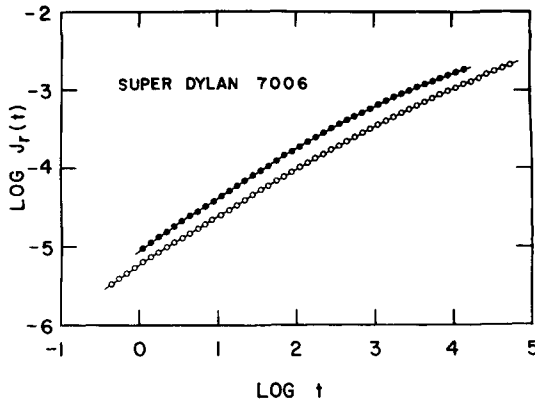


Fig. 7. Recoverable creep compliance curves $J_r(t)$ of high-density polyethylene, Super Dylan 7006 ($M_w = 1.25 \times 10^5$) measured at 138 and 180°C presented logarithmically as a function of time; $\sigma_m = 150$ dynes/cm²: (O) $T = 138^\circ\text{C}$; (●) $T = 180^\circ\text{C}$.

is due to the shorter preceding creep time, $\theta = 16.5$ hr. Judging from the appearance of the 138°C curve, the time to reach steady-state creep should be greater than several months.

The small effect of temperature on these materials is illustrated by the temperature dependence of the limiting low rate of shear viscosity η_0 of the Allied 55-100 HDPE, shown in Figure 8. Simple Arrhenius behavior is observed between 138 and 200°C with an apparent heat of activation of 7.5 kcal/mole.

In Figure 9, η_0 is logarithmically plotted as a function of the weight-average molecular weight. Since there is no apparent reason why linear HDPE shouldn't follow the usual 3.4 exponential dependence, we suspect that the large scatter and the deviation from the 3.4 line are a result of the presence of a small amount of long chain branching in some of the samples and consequent errors associated in calculating the molecular weight moments from GPC charts. The very presence of long-chain branches is known to enhance the viscosity at constant molecular weight.⁴ In addition, the presence of long-chain branches enhances the temperature sensitivity of the shear viscosity,³⁰ and it can be seen from Table II that values of $\eta(138^\circ\text{C})/\eta(180^\circ\text{C})$ for the Allied 55-100 HDPE and Super Dylan 6560 are 2.3 and 2.6, respectively. For SD 605 and SD 7006, the values are substantially higher, 2.9 and 5.9. The former are near the 3.4 line, and the latter are above it.

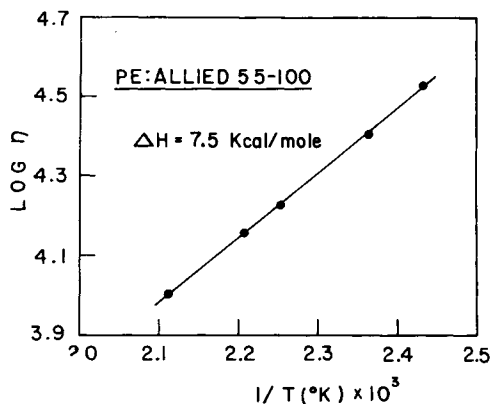


Fig. 8. Arrhenius plot of the temperature dependence of the limiting low rate of shear viscosity η of Allied 55-100 high-density polyethylene. An apparent heat of activation of 7.5 kcal/mole is indicated.

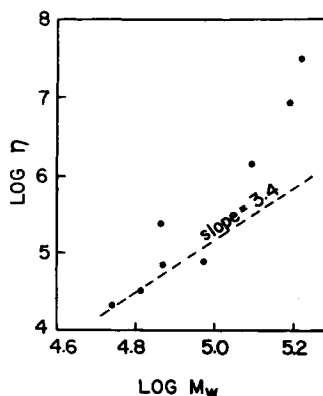


Fig. 9. Logarithmic plot of the limiting low rate of shear viscosity as a function of weight-average molecular weight of the high-density polyethylene samples studied at 138°C. The usual 3.4 slope is shown as a dashed line.

TABLE II
 High-Density Polyethylenes

Material	$\log M_w$	$\log \eta_{138^\circ\text{C}}$	$\log \eta_{180^\circ\text{C}}$	$\log J_e^a$	$\log (\eta^2 J_e)$	$\log \eta_{190^\circ\text{C}}^b$	B
Dow 18060	4.740	4.324		-3.74	4.91	3.886	1.53
Allied	4.813	4.529	4.156	-3.40	5.66	3.987	2.45
55-100							
SD 605	4.881	5.379	4.914	-2.54	8.22	4.415	1.85
SD 6550	4.869	4.847		-3.43	6.26	4.380	1.88
SD 6560	4.973	4.885	4.475	-3.21	6.56	4.255	1.78
SD 7007	5.097	6.162		-2.40	9.92	5.255	1.80
SD 7006	5.190	6.935	6.180	-2.0	11.87	5.279	1.71
SD 7002	5.238	7.487				5.756	1.45

^a Estimated except for the Dow 18060 value.

^b From Sabia¹⁴ fit to extrusion viscometer results.

These uncertainties are of little consequence with regard to our principal observations and conclusions. The 138°C recoverable compliance curves for all of the samples studied are presented in Figure 10. The associated creep stress σ_m for all of the curves was 150 dynes/cm². Therefore, the $J_r(t)$ curves reflect near-linear behavior for the lowest molecular weight samples. In addition, the departure of the higher molecular weight samples from linear behavior is deferred to longer times so that all of the curves represent linear behavior at times shorter than 10³ sec. Within the limits of knowledge of the molecular characterization of our samples there are no qualitative surprises. The steady-state recoverable compliance J_e of these HDPEs with broad molecular weight distributions does indeed increase with molecular weight. It is most sensitive to the high end of the distribution. Therefore, with comparable low molecular weight moments the sample with the highest M_z will have the highest J_e . Note that the order is Allied 55-100, SD 6560, and SD 605. The SD 605 has the lowest M_n but the highest M_z and therefore the highest J_e .

The order of the recoverable compliance curves along the time scale axis at short times clearly reflects the extent of the unseen rubbery entanglement plateau at still shorter times. The shifting of the terminal zone of response to longer times with increasing molecular weight, while the softening dispersions position on the time scale for a given kind of polymer only reflects the value of the glass temperature, is one of the unambiguously established facts in the viscoelastic literature.⁴ The relative position of the dispersion seen here preceding the terminal approach to J_e appears to be determined by the lower molecular weight moments M_n and/or M_w . The Dow 18060 looks like it has and should have the shortest rubbery plateau. The SD 605 apparently owes its appearance at short times to its low M_n . The responses of the Allied 55-100 and SD 6560 samples overlap, and they have the same M_n . However, the members of the SD 7000 series have M_n values comparable to each other and the other samples, and their positions appear to reflect their M_w values. The detailed effect of the molecular weight distribution awaits further study with model blends.

The most significant observation to be made that is germane to the motivation of this investigation is that the order of compliance levels of the HDPE samples has no meaning unless steady-state values are referred to. At different times of deformation preceding viscoelastic steady state, the order changes because the recoverable compliance curves cross as a result of the influence of the transient chain entanglement network.

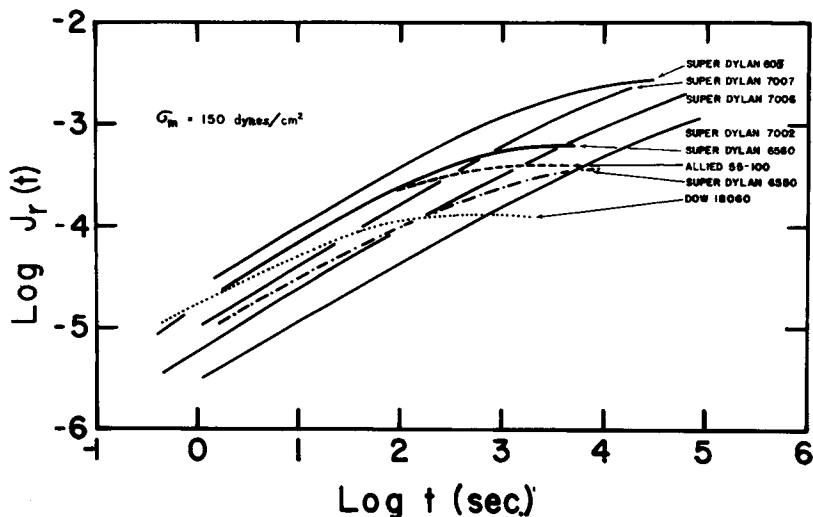


Fig. 10. Logarithmic plots of the recoverable compliance curves $J_r(t)$ of the eight linear polyethylenes studied shown as a function of time; measured at $\sigma_m = 150$ dynes/cm² and 138°C.

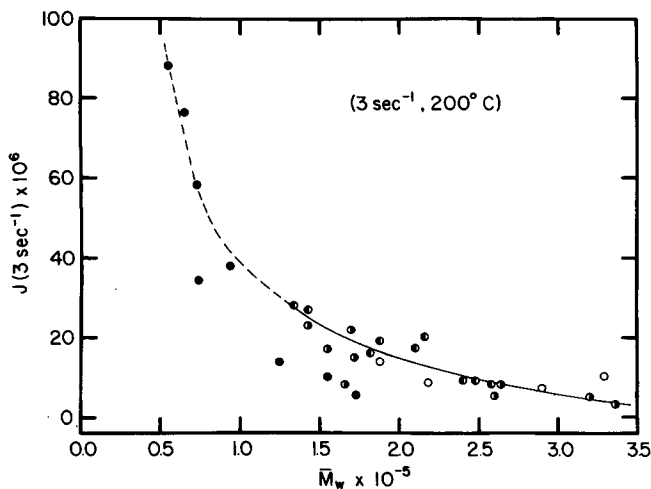


Fig. 11. "Shear compliance" calculated from die swell values obtained after extrusion at 200°C and subsequent annealing shown as a function of the weight-average molecular weight M_w . Calculations made using eqs. (11) and (12). Origin of points is indicated in the inset key: (●) this study; (◐) G samples (12); (◑) F samples (12); (○) WRG measured (12).

It is important to establish that the HDPE samples whose recovery response is shown in Figure 10 exhibit the same kind of anomalous "die swell" behavior as reported for the samples of Mendelson and Finger.¹² This has been done with the results shown in Figure 11 along with those of Mendelson and Finger from Figure 1 of reference 12. The annealed extrudate swell values $B = D/D_0$ obtained* following extrusion through a die with a diameter D_0 equal to 0.05 in. and a length-to-diameter ratio L/D_0 of 40 at 200°C are presented in Table II. The annealed diameter of the extrudate is D . Since the shear rate at the wall

* The extrusions were carried out by Anthony C. Jankowski.

was 3 sec^{-1} , our conditions were the same as those of Mendelson and Finger. Likewise, the "shear compliance" values plotted in Figure 11 have been calculated using eqs. (6) and (7) of reference 12:

$$S_R = (B^4 + 2/B^2 - 3)^{1/2} \quad (11)$$

and

$$J = \frac{3 S_R}{2 \tau_w} \quad (12)$$

where S_R is the average recoverable shear strain, J is the average shear compliance, B is the annealed swelling ratio. The shearing stress at the wall is τ_w . The swell ratio B values obtained on our samples after annealing at 140°C are listed in Table II. Although our J (3 sec^{-1}) values appear too low compared to the Mendelson-Finger results in the overlap region of the two sets of data, the decrease in J (3 sec^{-1}) with increasing molecular weight is clearly evident in the response of the samples being described here.

If one assumes an approximately constant capillary residence time for the polymers studied by Mendelson and Finger, the recoverable compliance curves in Figure 10 suggest an explanation for their "anomalous observations" on extrudate swell. Examination of isochronal recoverable compliance values reveals that at times far short of steady state, the molecular weight-compliance relationship is by and large inverted. The effect of higher rates of shear on $J_r(t)$ remains to be explored, but it does appear that viscoelastic steady-state conditions are not obtained on many polymers being extruded and therefore determined "die swell" values cannot be interpreted properly without additional information on the viscoelastic character of the polymer in question.

D. J. Plazek and N. Raghupathi would like to express their gratitude to the Engineering Division of the National Science Foundation for the financial support of their portion of the above research under Grant GK43292. The authors would also like to thank Linda Berardelli for her assistance with the calculations and figure preparations. Thanks are also due to Gerald R. Stich for some of the figures.

References

1. L. Boltzmann, *Sitzber. Kgl. Akad. Wien*, **70**, 275 (1874); *Ann. Phys.*, **7**, 624 (1876).
2. H. Leaderman, *Elastic and Creep Properties of Filamentous Materials and Other High Polymers*, Textile Foundation, Washington, D.C., 1943; in *Rheology*, Vol. 2, F. R. Eirich, Ed., Academic, New York, 1958, Chap. 1.
3. G. N. Lewis and M. Randall, *Thermodynamics and the Free Energy of Chemical Substances*, McGraw-Hill, New York, 1923, p. vii.
4. D. J. Ferry, *Viscoelastic Properties of Polymers*, 2nd ed., Wiley, New York, 1970.
5. D. J. Plazek and P. K. Agarwal, *Proc. VII International Congress on Rheology*, 1976, Gothenburg, Sweden, p. 488.
6. A. V. Tobolsky, J. J. Aklonis, and G. Akovali, *J. Chem. Phys.*, **42**, 723 (1965).
7. D. J. Plazek and V. M. O'Rourke, *J. Polym. Sci. A-2*, **9**, 209 (1971).
8. N. Raghupathi, Ph.D. Thesis, University of Pittsburgh, 1975.
9. W. W. Graessley, *Adv. Polym. Sci.*, **16**, 60 (1974).
10. B. D. Coleman, H. Markovitz, and W. Noll, *Viscometric Flows of Non-Newtonian Fluids*, Springer-Verlag, Berlin, 1966.
11. R. A. Stratton and A. F. Butcher, *J. Polym. Sci., Phys. Ed.*, **11**, 1747 (1973).
12. R. A. Mendelson and F. L. Finger, *J. Appl. Polym. Sci.*, **19**, 1061 (1975).
13. D. J. Pollock and R. F. Kratz, Sixth International GPC Seminar, Miami Beach, October, 1968.

14. R. J. Sabia, *J. Appl. Polym. Sci.*, **7**, 347 (1963).
15. D. J. Plazek, *J. Polym. Sci. A-2*, **6**, 621 (1968).
16. G. C. Berry, B. L. Hager, and C.-P. Wong, *Macromolecules*, **10**, 361 (1977).
17. H. Markovitz and G. C. Berry, *Ind. Eng. Chem., Prod. Res. Dev.*, **17**, 95 (1978).
18. C.-P. Wong and G. C. Berry, *Prepr. Am. Chem. Soc., Polym. Div.*, **15**, 126 (1974).
19. P. K. Agarwal and D. J. Plazek, *J. Appl. Polym. Sci.*, **21**, 3251 (1977).
20. D. J. Plazek and V. M. O'Rourke, unpublished work.
21. C.-P. Wong and G. C. Berry, *Polymer*, **20**, 229 (1979).
22. J. M. Simmons, *J. Sci. Instrum.*, **43**, 887 (1966).
23. R. I. Tanner and J. M. Simmons, *Chem. Eng. Sci.*, **22**, 1803 (1967).
24. M. Shida and R. N. Shroff, *Trans. Soc. Rheol.*, **14**(4), 605 (1970).
25. H. Markovitz, *Proceedings of the V International Congress on Rheology, Kyoto, 1968*, University of Tokyo Press, 1969, p. 499.
26. D. J. Plazek and N. Raghupathi, *J. Rheol.*, **23**, 477 (1979).
27. K. Ninomiya and J. D. Ferry, *J. Colloid Sci.*, **14**, 36 (1959).
28. D. J. Plazek, in *Methods of Experimental Physics: Polymer Physics*, R. A. Fava, Ed., Academic, New York, in press, Chap. 11.
29. E. Riande, H. Markovitz, D. J. Plazek, and N. Raghupathi, *J. Polym. Sci., Polym. Symp.*, **50**, 405 (1975).
30. W. W. Graessley, private communication.

Received January 15, 1979

Revised March 5, 1979